JOURNAL OF GEOPHYSICAL RESEARCH, VOL. 114, A01207, doi:10.1029/2008JA013722, 2009

Charge states of energetic ions in Jupiter's radiation belt inferred from absorption microsignatures of Io

R. S. Selesnick[1,2] and C. M. S. Cohen[3]

Received 3 September 2008; revised 4 November 2008; accepted 10 November 2008; published 15 January 2009.

[1] The Heavy Ion Counter on the Galileo Jupiter orbiter observed depletions of energetic ($\gtrsim$5 MeV/nucleon) oxygen and sulfur ions near Io that are interpreted as absorption microsignatures. The two elements were equally abundant in this region of Jupiter's radiation belt. Numerical simulations of microsignatures from Galileo orbits 27, 31, and 32, based on calculations of ion trajectories in models of the magnetospheric and Alfvén wing magnetic fields, show that the data are most consistent with the ions being fully ionized or nearly so. The conclusion is independent of field model inaccuracies, which cause some discrepancy between simulations and data, because the Alfvén wing field significantly deflects only those trajectories with relatively small gyroradii.

Citation: Selesnick, R. S., and C. M. S. Cohen (2009), Charge states of energetic ions in Jupiter's radiation belt inferred from absorption microsignatures of Io, *J. Geophys. Res.*, *114*, A01207, doi:10.1029/2008JA013722.

1. Introduction

[2] Radiation trapped in Jupiter's inner magnetosphere includes an abundance of heavy ions, predominantly oxygen and sulfur with some sodium [*Krimigis et al.*, 1979a, 1979b; *Vogt et al.*, 1979a, 1979b]. The presence of sulfur and sodium implies that the ions' origin is the surface or atmosphere of Io, but radial density gradients show that they actually arrive from a distant source well beyond Io's orbit [*Gehrels and Stone*, 1983; *Cohen et al.*, 2000]. The accepted explanation has been that charge exchange in the Io plasma torus produces fast neutral atoms that escape to the outer magnetosphere where a small fraction are reionized by solar UV radiation or electron impact. Some are then accelerated by plasma waves and by inward diffusion, reaching energies $\sim$10 MeV/nucleon as they arrive back in the inner magnetosphere [*Barbosa et al.*, 1984].

[3] The theory predicts that the radiation belt energetic ions originating from Io should be singly ionized, in contrast to the ions of solar origin observed in Jupiter's middle magnetosphere that are expected to be in high charge states [*Cohen et al.*, 2001]. Lower-energy ions have been observed in several charge states (+1 to +4 for both O and S), in the Io torus itself for energy-per-charge up to 6 kV [*Bagenal*, 1994] and in the middle magnetosphere for up to 60 kV [*Geiss et al.*, 1992], but these are not thought to be the source of the radiation belt ions. While several measurements of the trapped energetic ion intensity have been made, the charge states have not been experimentally determined. However, detailed observations from the Galileo orbiter of depletions in the ion intensity caused by Io itself provide an opportunity for indirect assessment of the ion charge states.

[4] Absorption signatures of moons in planetary magnetospheres have been studied previously for their utility in determining trapped particle transport rates, properties of the planetary magnetic fields, and properties of the moons themselves [e.g., *Thomsen*, 1979; *Chenette and Davis*, 1982; *McKibben et al.*, 1983; *Hood*, 1989; *Selesnick*, 1992, 1993; *Paranicas and Cheng*, 1997]. They have been broadly divided into two categories: macrosignatures are large-scale depressions in radial intensity profiles caused by particle absorption averaged over many orbits of the moon; microsignatures are small-scale depletions caused by recent passage of the moon through a particle population. Often a microsignature is superimposed on the broader macrosignature, as has been observed near Io [*Cohen et al.*, 2000].

[5] In this work we are concerned with microsignatures observed by the Heavy Ion Counter (HIC) on Galileo during three close passes by Io in 2000 and 2001. As a consequence of passing within 200 km of Io's surface, and of the high time resolution available, considerable structure was seen in each microsignature. Interpretation of these data requires detailed understanding of the local ion populations and of the motion of individual ions through the local magnetic field. Our goal is to construct a realistic model of the microsignature formation, then vary the ion charge states within the model to determine their values by comparison with the data.

2. Ion Data

[6] Microsignatures were observed by HIC at close encounters with Io during Galileo orbit numbers 27, 31, and 32. The encounter dates and other pertinent information are listed in Table 1; the trajectories past Io are illustrated in Figure 1. In each case Galileo passed Io in a direction, referring to the corotating magnetospheric plasma, from upstream to downstream; it passed near Io's equatorial plane

[1]The Aerospace Corporation, Los Angeles, California, USA.
[2]Now at Los Angeles, California, USA.
[3]California Institute of Technology, Pasadena, California, USA.

0148-0227/09/2008JA013722$09.00

Table 1. Io Encounter Parameters[a]

Orbit	Date	UT Hour	h	L	λ	J	γ	n
27	22 Feb 2000	13.78	198	5.94	−4.7	8.5	−7	0.50
31	6 Aug 2001	4.99	193	5.90	7.5	4.5	−7	0.28
32	16 Oct 2001	1.39	184	6.01	4.8	5.5	−7	0.40

[a]Minimum distance h in km from the surface of Io; L shell and magnetic latitude λ for Jupiter's dipole magnetic field; local O or S ion intensity $J\left(\frac{E}{10\text{MeV/nuc}}\right)^{\gamma} \sin^n \alpha$ in $(\text{cm}^2\ \text{s sr MeV/nuc})^{-1}$.

in orbit 27, over the north pole in orbit 31, and over the south pole in orbit 32.

[7] Two types of data were collected by HIC during the encounter intervals. The "rate" data contain the total number of particles that triggered required detector combinations during every 2 s interval. They provide high-resolution, nearly continuous ion flux time series. A subset of the same particles are also included in the "event" data, for which the energy deposits in each detector were recorded. By later analysis they provide composition and spectral information.

[8] During the Io encounter orbits the HIC LETB sensor was configured to trigger on two- or three-detector coincidences, resulting in energy ranges of 4.3 to 18.5 MeV/nucleon for O ions and 5.6 to 26.1 MeV/nucleon for S ions [*Garrard et al.*, 1992]. The resulting rate data, or ion fluxes, from the three encounter intervals are shown in Figure 2. Typically they are modulated by Galileo's rotational period of 19 s. Early in each encounter interval there are two flux maxima per rotation corresponding to the two instances in which LETB is oriented to view particles arriving from directions perpendicular to the local magnetic field. Later this is modified by the presence of Io with instances in which only one flux maximum per rotation is evident. Clear broad decreases in the flux for periods ~0.2 h are roughly consistent with intervals during which Galileo passed across the disk of Io (Figure 1).

[9] To study the effects of Io it is necessary to first determine the unmodified ion distribution functions. We assume that the ion pitch angle distribution (PAD) is proportional to $\sin^n \alpha$, where α is the pitch angle relative to the local magnetic field and n is a constant to be determined by the modulation of the rate data just prior to each encounter interval. This is done by Monte Carlo simulation: At intervals along the Galileo orbit directions are randomly sampled from a PAD with an assumed n (the magnetic field direction is from the magnetospheric field model described below). Then each direction is associated with a location obtained by random sampling from a uniform distribution on the front detector face within the LETB aperture. Then it is determined for each case whether the geometrical requirements for a LETB trigger are satisfied. The rate of such triggers are tabulated with 2 s averages for comparison with the rate data. The process is repeated with varying n values to find the best possible match.

[10] The composition and energy spectra were determined from LETB and LETE event data [*Garrard et al.*, 1992]. For each orbit they were divided into three ~20-min periods from just prior to, during, and just after each encounter. Results for all of the time periods were consistent with the O and S ions having equal abundance and common power law energy spectra of the form E^{γ} where E is kinetic energy per nucleon. The normalization factor J, defined as the O or S ion intensity for $\alpha = 90°$ and $E = 10$ MeV/nucleon, varies between orbits and is listed in Table 1, as are γ and n. Owing to statistical limitations the intensities calculated from the event data were generally uncertain to within a factor ~2, but the normalization of the total ion flux by the rate data is accurate to $\lesssim$10%.

[11] The n values are positive and thus J, the local perpendicular ion intensity, should decrease with increasing magnetic latitude as a greater fraction of the ion population mirrors at lower latitude. However, the magnetic latitude differences between the three encounters are much too small to account for the different J values, which are also not ordered by the small differences in L value (Table 1). Therefore it appears that the changes in J and n between the encounters are due to time variability rather than spatial gradients. The data show that their values are relatively steady during each encounter interval and we assume them

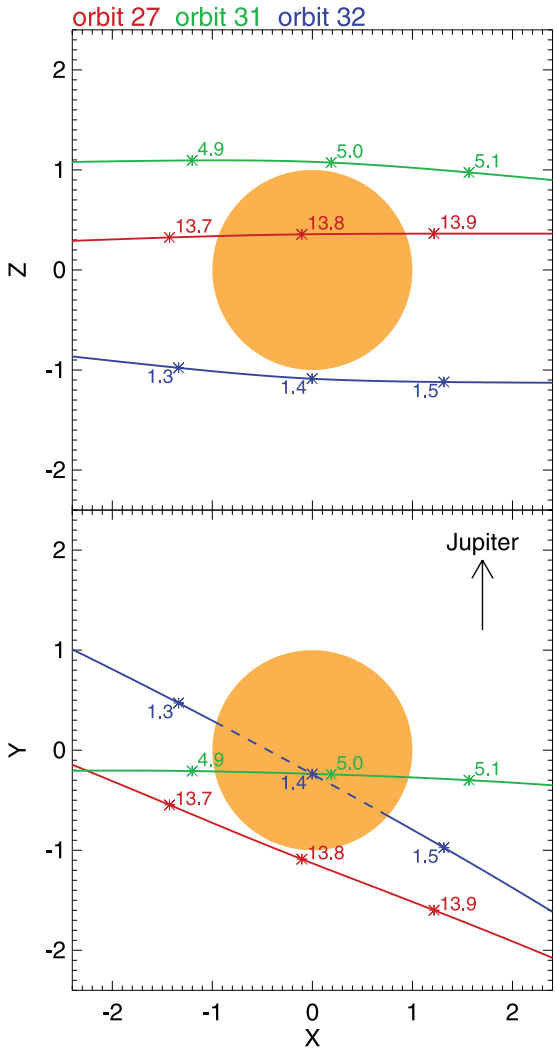

Figure 1. Galileo trajectories past Io labeled with time in hours (UT). Dimensions are in Io radii (1821.5 km), and the coordinate system is centered on Io with Z parallel to Jupiter's rotation axis, Y toward the rotation axis, and X in the rotation direction.

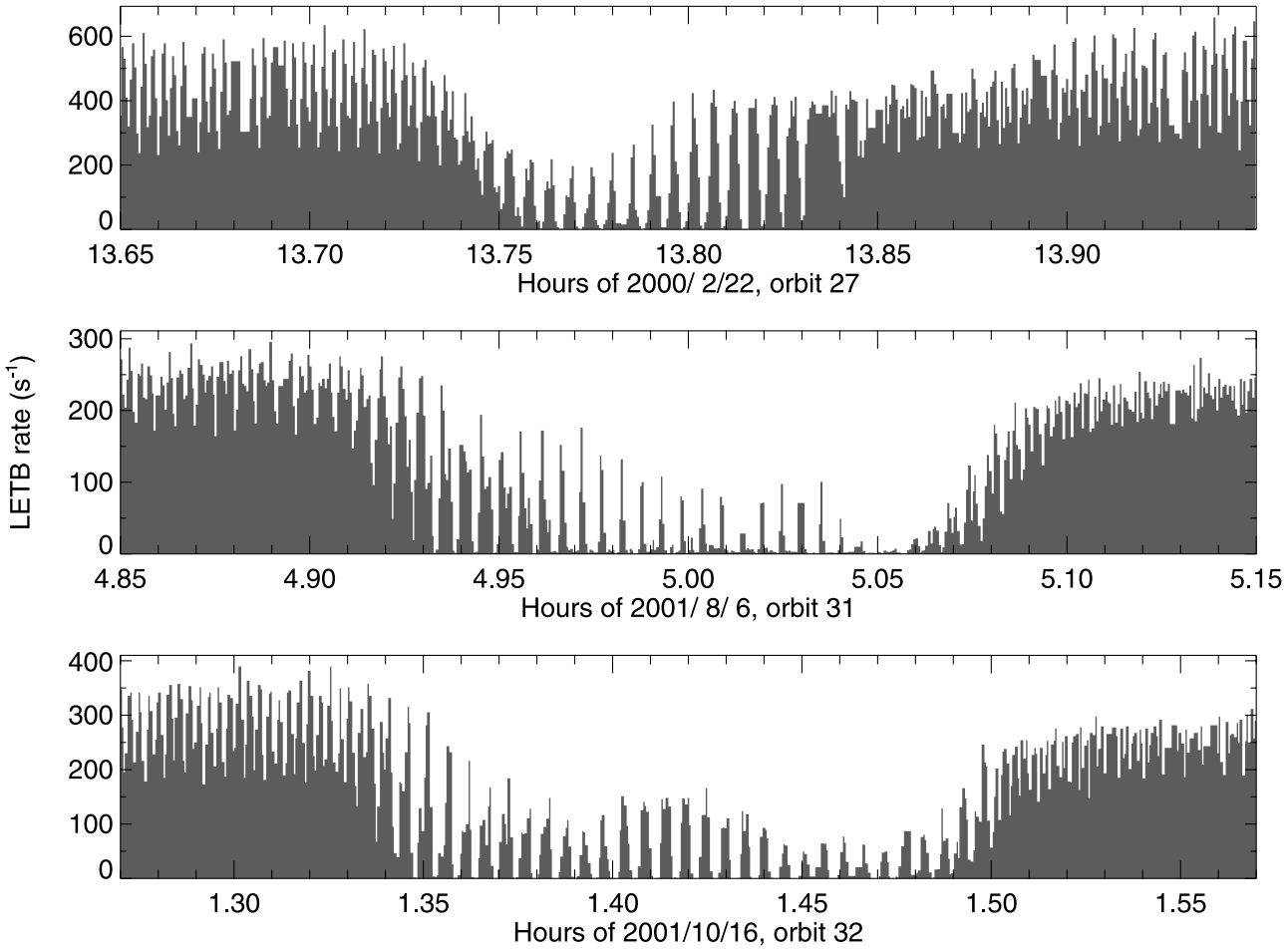

Figure 2. Ion flux versus time measured on Galileo by HIC/LETB from the three Io encounters.

to be constant. While the derived composition, energy spectra, and pitch angle distributions are undoubtably simplified versions of reality, they are sufficient inputs to the microsignature simulations for accurate results to be obtainable, as we have verified by sensitivity tests.

3. Microsignature Simulations

[12] The Io microsignatures as seen in the LETB rate data are simulated by extending the calculation, described above, that was used to determine the unmodified ion pitch angle distributions. At points along the Galileo orbit ion arrival directions are found that satisfy the LETB trigger requirements, as before. Now it must be determined whether these directions correspond to ion trajectories that have not recently passed through the solid body of Io. Only then are they included in the simulated rate data. The existence of trajectories that recently did pass through Io thereby reduce the simulated rate and form the predicted microsignature. By following the trajectories backward in time from their arrival at Galileo it is necessary to calculate the trajectories only of ions that satisfy the trigger requirements.

[13] The shape of an ion trajectory depends on its rigidity, or momentum per charge, an initial position, and an initial direction (for time reversed trajectories final conditions are used instead of initial ones). The speed along the trajectory is also required to compare the ion location at each time step with that of Io. Therefore, in addition to sampling the ion arrival directions from the known pitch angle distribution, the energy and type of ion must be sampled from the known energy spectra and composition. Trajectories are entirely equivalent for ions having both common charge to mass ratios and common speed (or common kinetic energy per nucleon, E). Therefore ^{16}O and ^{32}S ions with equal E are equivalent if the S charge state is double the O charge state. However, because LETB is sensitive to somewhat different ranges of E for O and S it is necessary to include each ion component in the simulation.

[14] Though trapped ions are confined to common drift shells regardless of energy or rigidity, whether ions on a drift shell that intersects Io's orbit actually collide with Io is strongly dependent on whether the ion gyroradius is larger or smaller than the Io radius, and therefore so is the shape of the observed microsignature. For O and S at LETB energies the gyroradii are larger than Io for the low ion charge states and smaller than Io for the high ion charge states (6 MeV/nucleon O^+ and O^{+8} have gyroradii $\sim$3200 and 400 km, respectively; Io's radius is 1821.5 km). Therefore, the observed microsignatures provide strong constraints on the actual charge states. To apply them the simulations are carried out separately for each charge state of each component and

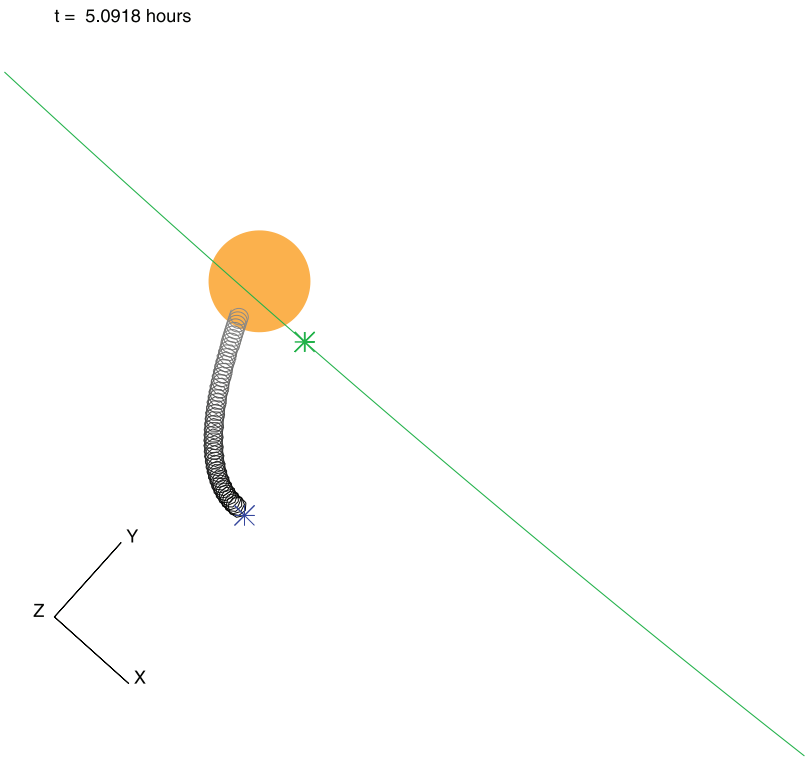

Figure 3. Frame from Animation S1 of a sample 6 MeV/nucleon O^{+8} ion trajectory in orbit 31 projected on the *X*-*Y* plane of Figure 1. The blue symbol is at the present location of the ion with prior locations shown by the spiral curve. The Galileo trajectory is in green with the symbol showing its present location. The ion trajectory was calculated backward in time starting from the Galileo position at t = 5.1 h. Only the magnetospheric field model was included.

then various linear combinations of the results are taken for comparison with the data.

3.1. Magnetic Field

[15] As Galileo rotates and the LETB view direction changes the ion arrival directions vary through the full range of pitch angles. The time reversed ion trajectories may travel substantial distances along magnetic field lines before returning to the vicinity of Io within a short interval. Therefore, a model of the large-scale magnetic field is required to calculate the trajectories. However, details of the magnetic field at large distances are not critical, just the return of the ion to Io's vicinity. For example, high-order multipole components of Jupiter's magnetic field influence ion trajectories as they approach Jupiter, but the return to Io is controlled largely by the dipole component. Similarly, details of the magnetospheric current sheet magnetic field are insignificant. These conclusions have been verified by calculating trajectories in large-scale magnetic field models of varying complexity. For the final simulations a simple model was adopted that combines Jupiter's dipole field with a uniform current sheet field. We call this the magnetospheric field model.

[16] Ion trajectories may also be influenced by the small-scale magnetic field formed by the interaction between Io and the plasma torus [*Neubauer*, 1980]. Currents are generated that flow along standing MHD waves in Io's rest frame, called Alfvén wings, extending far from Io and closing through the ionosphere or solid body of Io. The magnetic field of the Alfvén wings is extended but its influence is small scale in the sense that trajectories must pass near the wing to be significantly influenced. Similarly, trajectories must pass near Io to be influenced by the magnetic field of the currents flowing within Io or its ionosphere.

[17] Trajectories passing near the small-scale magnetic field can be deflected from the path that they would otherwise follow. The location of the Alfvén wings and details of the small-scale field are critical in determining its precise influence. However, the influence is only significant for high charge state ions because those with low charge state again have gyroradii larger than the scale of the field which is similar to the radius of Io. Therefore, if the ions have high charge states then a model of the small-scale magnetic field is required. Unfortunately one is not readily available. Though detailed calculations of the local field around Io have been carried out [*Saur et al.*, 2002] the locations and current distributions of the Alfvén wings depend on the extended properties of the plasma torus and are not well known. Complications such as reflection and refraction at plasma density gradients also exist. Despite these difficulties we have adopted a relatively simple model of the small-scale magnetic field that is derived from currents flowing in a cylindrical 2-dimensional dipole configuration on Alfvén wings extending north and south from Io, with additional closure currents around Io at the end of each cylinder. We call this the Alfvén wing model, though it also includes the field of the closure currents. The model is parameterized by an Alfvén Mach number M_A. Various values of this parameter have been tested and we settled on M_A = 0.2 as a reasonable value that is within the

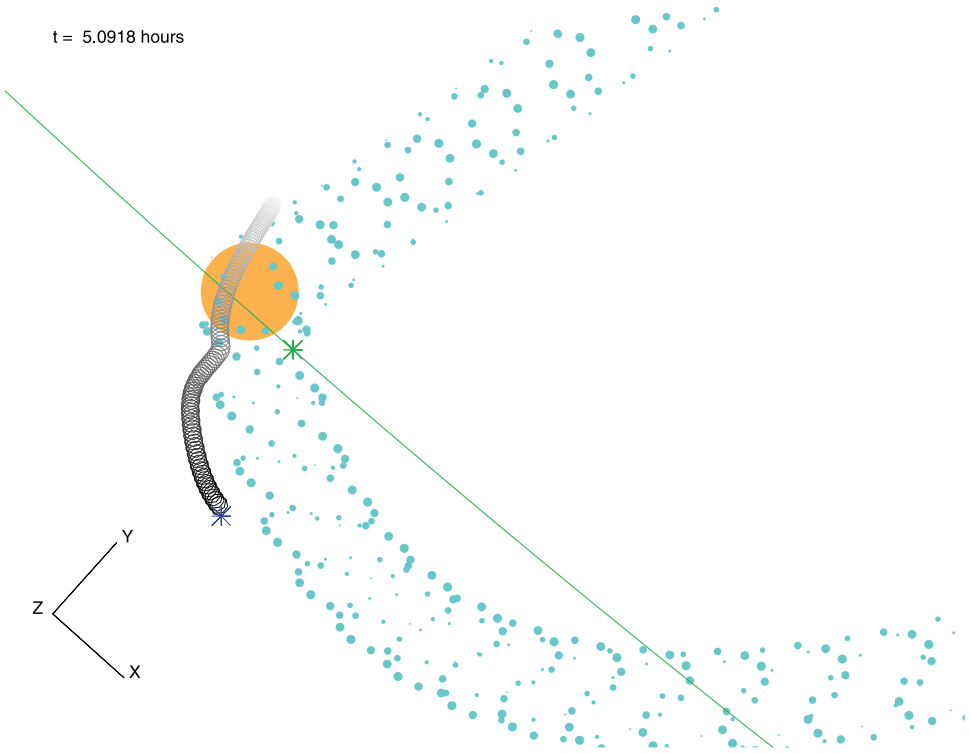

Figure 4. Similar to Figure 3 but calculated with the Alfvén wing model in addition to the magnetospheric field model. Light blue dots represent the Alfvén wing currents, their size (and speed in Animation S2) being proportional to the current magnitude.

range (0.16 to 0.39) derived from plasma and field measurements [*Kivelson et al.*, 2004]. The simplicity of the model precludes the determination of a M_A value that provides a best fit to the data. Nevertheless, the model is adopted in order to test its influence on the microsignature simulation and to reach any conclusions that may be independent of the model accuracy. Far from Io the Alfvén wing model is similar to the 2-dimensional dipole field that was suitable for modeling observations of magnetic perturbations during the Voyager mission [*Acuña et al.*, 1981]. Details of both the magnetospheric field and Alfvén wing models are described in Appendix A.

3.2. Sample Ion Trajectories

[18] After the final conditions of an ion trajectory entering the LETB aperture are determined by random sampling from the known distribution functions, the prior trajectory is calculated by integrating the equation of motion backward in time. The integration is carried out in the rotating System III coordinate system and the only force term in the equation of motion is that of the model magnetic field. The integration is continued until the trajectory collides with Io, or until the time reversed drift motion is increasing the distance from Io so that they cannot have collided within the most recent drift orbit. If there is a collision it means that the trajectory recently intersected Io and it is assumed to be unpopulated by ions.

[19] Two sample trajectories are represented in auxiliary material[1] Animations S1 and S2, single frames of which are also shown in Figures 3 and 4. The trajectories both were calculated for 6 MeV/nucleon O^{+8} and with the same final conditions at Galileo, differing only in that the first was calculated with the magnetospheric field model alone while the second also includes the Alfvén wing model. In the first case the trajectory recently intersected Io while in the second case it was deflected around Io by the Alfvén wing field.

3.3. Results

[20] Many trajectories of the type described above were calculated to simulate the LETB rate data for each encounter interval and each ion charge state, with and without the Alfvén wing model. Results are shown in Figures 5, 6, and 7 for orbits 27, 31, and 32, respectively. For each orbit, simulations with four combinations of single O and S charge states are included: O^{+} and S^{+}; O^{+2} and S^{+4}; O^{+4} and S^{+8}; O^{+8} and S^{+16}. These clearly show changes in the simulated microsignatures, and the increasing influence of the Alfvén wing model, as the charge states increase. Other combinations of charge states can be made by simple linear combinations of the results but do not provide additional insight.

[21] We first consider results for orbit 31 (Figure 6) in which Galileo passed over the north pole of Io at northerly magnetic latitude. For singly charged ions, with gyroradii larger than Io, the simulations with and without the Alfvén wing model are similar as expected, small differences being partly due to the Monte Carlo statistics. At the start of the interval the simulated flux minima, both with and without the Alfvén wing model, are greatly reduced relative to those in the data, which is a result of the large gyroradius

[1] Auxiliary materials are available in the HTML. doi:10.1029/2008JA013722.

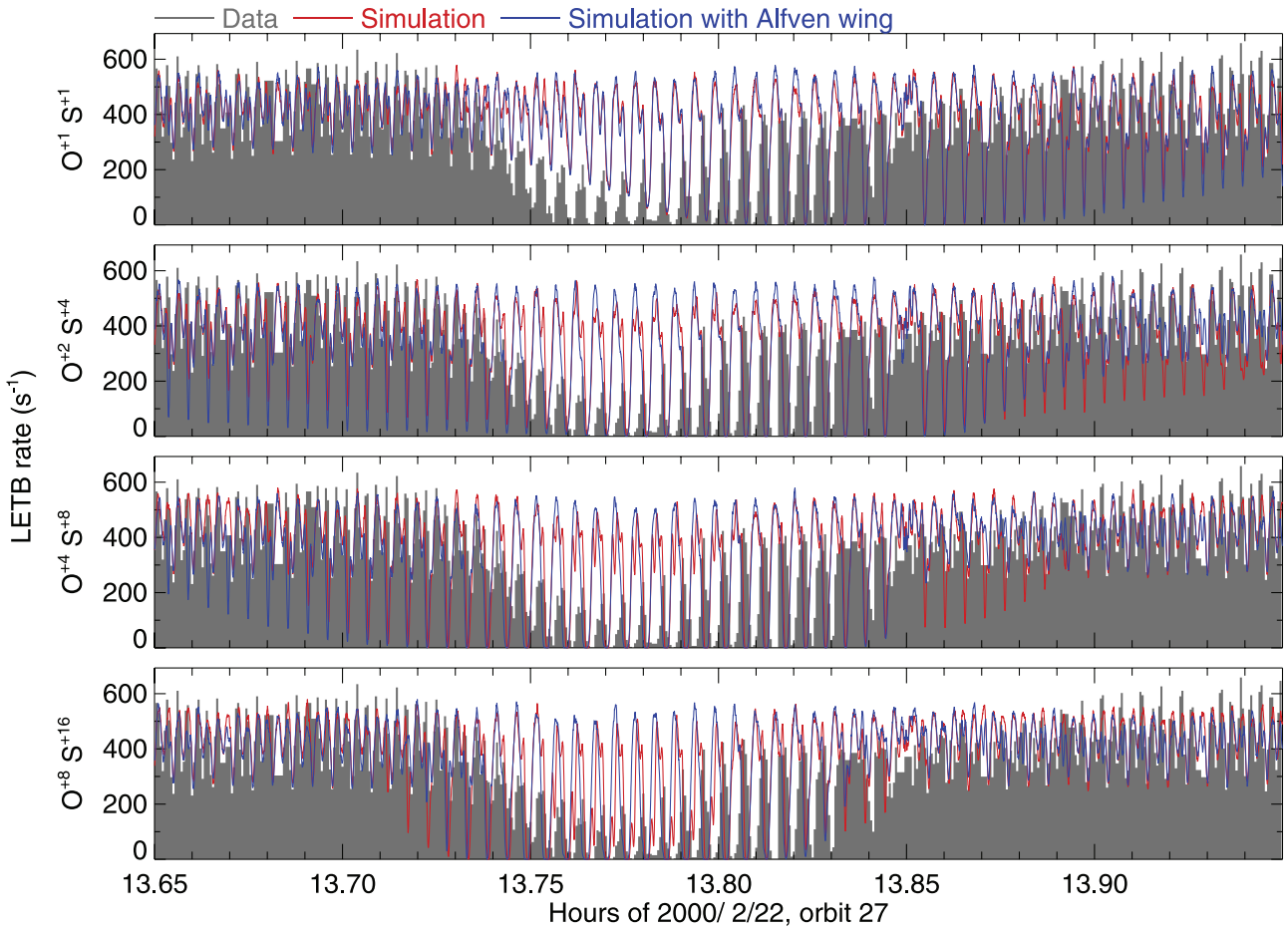

Figure 5. Ion flux versus time from orbit 27 data (gray) and from simulations without (red) and with (blue) the Alfvén wing model. The simulations are shown for various ion charge states. The data are the same in each case and repeated from Figure 2 for comparison with the simulations.

extending the trajectories ahead of Galileo as it approaches Io. For the higher charge states the gyroradii decrease and the trajectories cannot reach Io until Galileo is closer to it, so the flux minima prior to the encounter are shallower.

[22] The flux maxima for singly charged ions are at a nearly constant level throughout because their trajectories must be at a certain gyrophase to collide with Io. The gyroradii for higher charge states can be small enough that a collision is inevitable regardless of gyrophase and so even the flux maxima decrease near Io.

[23] For higher charge states the simulations with and without the Alfvén wing model diverge as Galileo reaches and passes Io. The difference is greatest for the fully ionized case after Galileo has passed by Io (hour $\gtrsim$5.05), when the simulation without the Alfvén wing predicts rates near zero while the simulation with the Alfvén wing predicts rates that are nearly unmodified by Io in close accord with the data. This is the case illustrated by Figures 3 and 4 in which a trajectory that would have otherwise collided with Io is deflected away by the Alfvén wing field. Without the Alfvén wing, nearly all of the trajectories from this period passed through Io prior to reaching Galileo, though they may have mirrored one or more times in between. With the Alfvén wing nearly all of the trajectories were deflected away from Io.

[24] Results from orbit 32 (Figure 7) are similar to those from orbit 31 because they were both polar passes at northerly magnetic latitude (though orbit 32 was over Io's south pole this does not to cause a significant difference). The approach velocity of Galileo in orbit 32 included a radial component relative to Jupiter, rather than being nearly azimuthal as in orbit 31, so that near the start and end of the encounter interval Galileo was on drift shells that were further from Io's orbit than at the equivalent times in orbit 31. This caused the flux minima at the start of the interval for the singly ionized case to be unmodified by Io and similarly for the fluxes in the fully ionized case without the Alfvén wing at the end of the interval.

[25] Results from orbit 27 (Figure 5) are quite different than those from the other two orbits because it is a low latitude rather than polar pass (Figure 1). Differences between the simulations with and without the Alfvén wing model are small even for the high charge state ions because the Galileo orbit does not pass near either Alfvén wing. Flux maxima are never substantially modified by Io for any charge state, in contrast to the data for which the maxima are substantially reduced during hours $\sim$13.75 to 13.8. This may be indicative of unmodeled magnetic fields caused by currents flowing within Io or its ionosphere. The main distinction between the different charge state

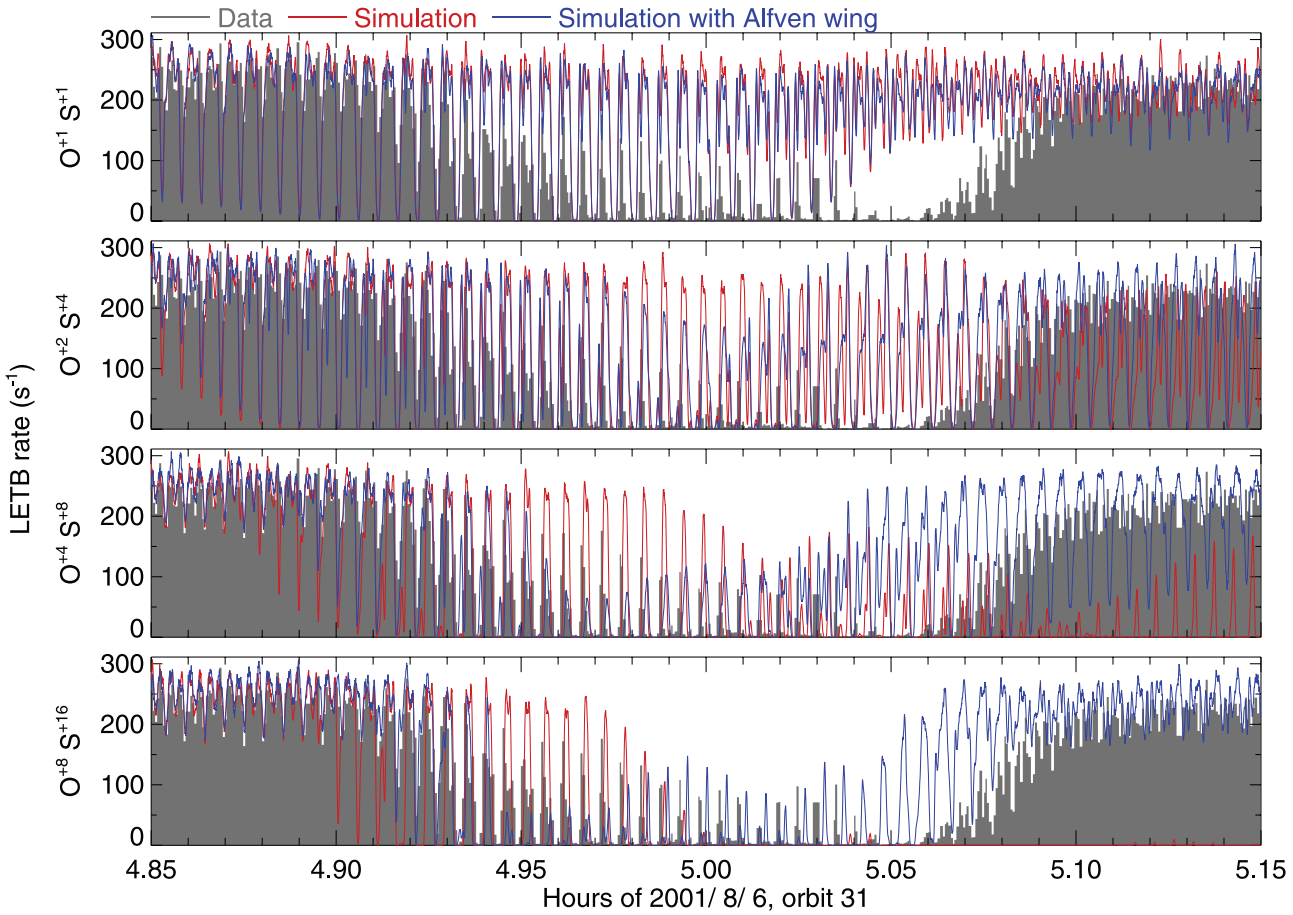

Figure 6. Similar to Figure 5 but for orbit 31.

simulations for this orbit is in the variations of the flux minima both early and late in the encounter interval. For the lower and intermediate charge states these are substantially reduced, at least before or after the encounter, while in the fully ionized case and in the data they are reduced only near Io.

4. Conclusions

[26] The results of the simulations described above lead to several conclusions regarding the interpretation of the microsignature data in general and the ion charge states near Io in particular:

[27] The microsignatures are not sensitive to details of the magnetospheric field model. A simple dipole model with uniform current sheet field is sufficient. If the trapped ions have low charge states (O^+, S^+) then they also are not sensitive to the Alfvén wing field; the simulated microsignatures are the same with or without that field and they do not fit the data. Therefore, assuming that we have accounted for all significant influences on the ion trajectories, the ions cannot have low charge states.

[28] With higher charge states the simulated microsignatures for the high-latitude passes of orbits 31 and 32 are strongly influenced by the Alfvén wing field and the fits to the data are improved despite the simplicity of the field model. Therefore, the data are most consistent with high ion charge states and the fits appear to be best for charge states at or near their maximum values (O^{+8}, S^{+16}). The same is true for orbit 27, though to a lesser extent because of a greater discrepancy between data and simulations. We expect that a more accurate model of Io's local magnetic field would improve the fits for all three orbits, particularly for orbit 27, where the field should have greater relative influence due to the low latitude of Galileo, and for the latter part of orbit 32.

[29] Further support for high charge states is obtained from orbit 31 when Galileo is just upstream of Io prior to the encounter. The observed ions have not yet been strongly influenced by the Alfvén wing field (the wings extend downstream), so the simulated microsignatures from this region are nearly independent of the Alfvén wing model. Only the high charge state simulations fit the data from this region. In orbit 27 a similar conclusion is reached from the data downstream of Io.

[30] By deflecting particle trajectories the Alfvén wing field acts as a local scattering center associated with Io. It is possible that scattering by plasma waves associated with the passage of Io through the local torus plasma could have a similar influence on the shape of the ion microsignatures, but the Alfvén wing is known to exist and so we did not attempt to include any other local scattering mechanisms in the simulations. The scattering is only effective on ions with high charge states because the gyroradius must be small enough that the ion trajectory remains in the vicinity of the Alfvén wing, as verified by the simulations.

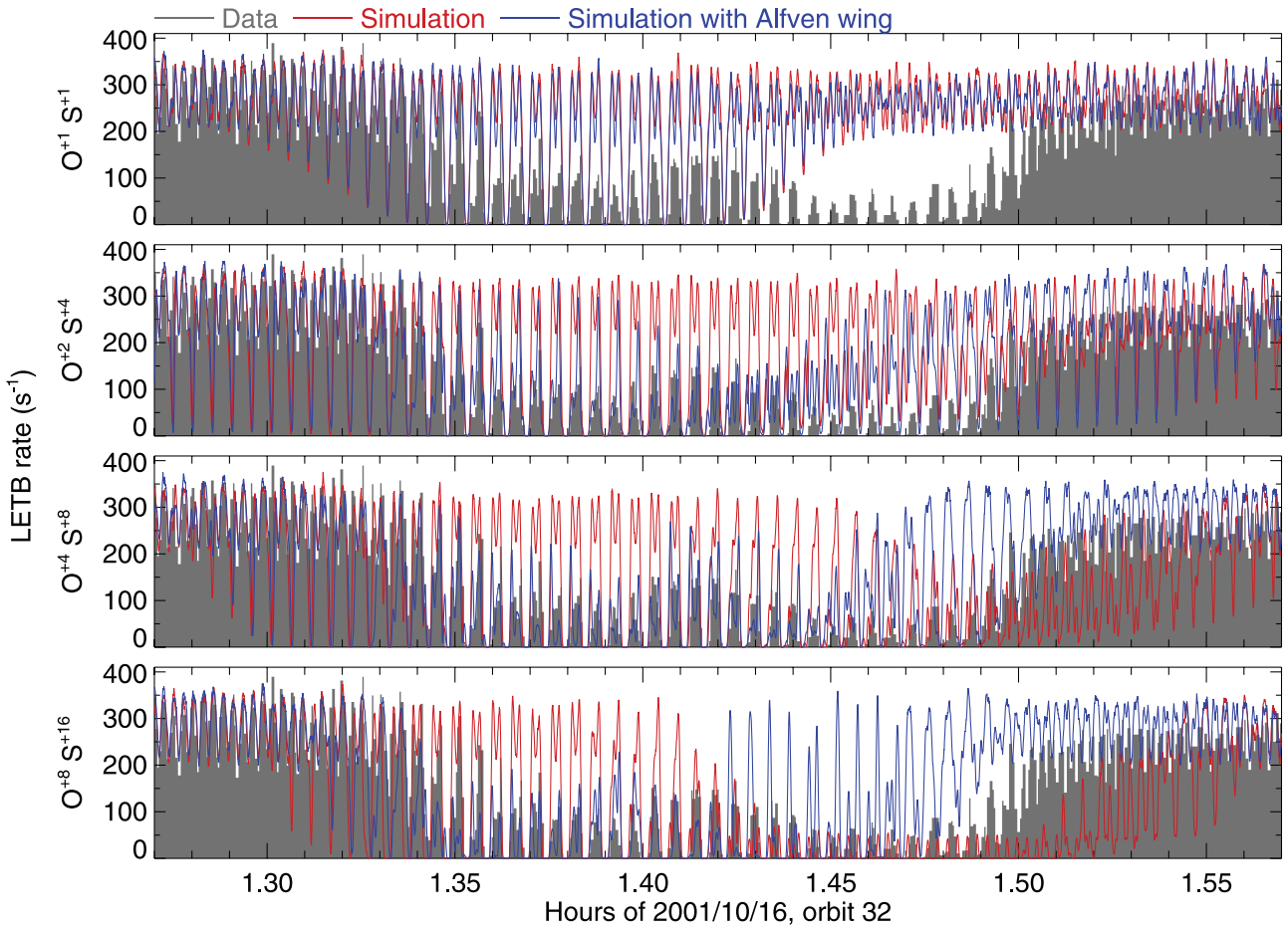

Figure 7. Similar to Figure 5 but for orbit 32.

[31] Scattering could be effective for low charge states if it occurred over a much larger region of space. Radial diffusion transports ions inward but it is unlikely to be significant in the short time intervals ($\lesssim$1 min) during which the ion trajectories travel between Io and Galileo. Even so, such scattering that is unrelated to the presence of Io leaves ions with nearly the same gyroradii and on drift shells with nearly the same radial extent, so it cannot significantly modify the simulation results. We have verified this conclusion by adding scattering to the trajectory calculation. This was done by randomly modifying the direction of the trajectory at each time step to simulate scattering with a constant rate that is uniform in space. Different rates were tried but the simulations were substantially unmodified from those without scattering. In particular, the large gyroradii of ions with low charge states means that they still reach Io ahead of Galileo, forming deep minima in the simulation that are not seen in the data (see, for example, the top of Figure 6). If scattering was somehow fast enough to fill in the deep minima seen ahead of Io, then it would also eliminate the modulation caused by the PAD away from the microsignature and it would probably substantially eliminate the microsignature itself (though we have not tested this case by simulation).

[32] A subtle limitation of the simulations is that they cannot account for scattering that may modify the ion PAD, because arrival directions are sampled from a constant PAD prior to the trajectory tracing. Reduced modulation in data after the orbit 31 and 32 encounters (last $\sim$0.05 h in Figure 2) may be caused by scattering, or deflection, from the Alfvén wing, as is necessary to reproduce the average flux level observed in that region. However, the PAD modulation is minor compared to the microsignature itself and so the conclusions regarding charge states are unaffected.

[33] The Alfvén wing model is highly idealized and leads to inaccuracies that are particularly evident for orbit 27. However, the determination that the ion trajectories are significantly modified by the Alfvén wing model was sufficient to conclude that high charge states are required for accurate simulation. We are unaware of any mechanism that could modify the trajectories of low charge state ions sufficiently to make them consistent with the observations. The conclusion that the ions are in high charge states should be considered in evaluating theories of their origins.

[34] Earlier conclusions that energetic ions originating from Io are singly ionized were based on observed abundance ratios near Io itself [*Garrard et al.*, 1996] and in the middle magnetosphere [*Cohen et al.*, 2001]. These were qualitative arguments seen to confirm the theory for reionization of fast neutrals. In light of the present results derived from microsignature simulations, the earlier conclusions should, perhaps, be reexamined. Complementary simulations of the large-scale macrosignatures could provide an opportunity to do so, by predicting quantitative changes in

abundance ratios caused by Io absorption as a function of ion charge state.

Appendix A: Magnetic Field Models

A1. Magnetospheric Field Model

[35] Jupiter's dipole magnetic field has moment 4.28 GR_J^3 tilted 9.6° from the rotation axis toward longitude 201.7° W and offset from the center of the planet by 0.131 R_J toward latitude 8.0° S, longitude 148.57° W [*Acuña and Ness*, 1976]. This is combined with a uniform current sheet magnetic field of 0.00192 G directed parallel to Jupiter's rotation axis and reducing the total equatorial field magnitude. The magnitude of the current sheet field is from Galileo measurements (K. Khurana, private communication, 2007).

A2. Alfvén Wing Model

[36] The tangent to the Alfvén characteristic, or Alfvén wing direction, is

$$\mathbf{t} = \pm\mathbf{b} + M_A\mathbf{c} \tag{A1}$$

where M_A is the Alfvén mach number, **c** is a unit vector in the plasma corotation direction, **b** is a unit vector in the direction of the background (magnetospheric) field, and the ± is for propagation parallel or antiparallel to **b** (south or north of Io). This equation is integrated to obtain the paths of the Alfvén wings as they propagate away from Io. Variations in M_A and reflections at the boundary of the plasma torus are neglected.

[37] The current that generates the field of one Alfvén wing flows on the surface of a cylinder with radius $a = 1.05R_{Io}$ (Io radii) that is centered on the Alfvén characteristic, and closes along the end of the cylinder that is a circle centered on Io. We use cylindrical coordinates with the origin at Io, z along the Alfvén wing, cylindrical radius R, and azimuthal angle ϕ measured from the direction $\mathbf{t} \times \mathbf{r}$ of the 2-d dipole moment, where **r** is a vector from Jupiter to a position on the Alfvén wing. Then the current density is

$$\mathbf{J} = i_0\delta(R-a)\big(\sin\phi\Theta(z)\mathbf{e}_z + a\cos\phi\delta(z)\mathbf{e}_\phi\big) \tag{A2}$$

where δ is the Dirac delta function, Θ is the unit step function, $\mathbf{e}_z$ and $\mathbf{e}_\phi$ are unit vectors in the z and ϕ directions, respectively, and the maximum surface current density is

$$i_0 = \frac{\mu c}{2\pi a^2} \tag{A3}$$

The 2-d dipole moment magnitude is [*Neubauer*, 1980]

$$\mu = \frac{Ba^2M_A}{\sqrt{1+M_A^2}} \tag{A4}$$

where $B = 0.02$ G is the approximate equatorial background magnetic field magnitude.

[38] The cylindrical components of the magnetic field are obtained from **J** by integration using the Biot-Savart law and neglecting the curvature of the Alfvén wing:

$$B_R = \frac{\mu\cos\phi}{2\pi a^2R^2st^2}\Big(z\big[a^2+R^2+z^2\big]^2E(m) - t^2\Big[-\pi sx_<^2 + z^3K(m) + (a-R)^2z\Pi(n|m)\Big]\Big) \tag{A5}$$

$$B_\phi = \frac{\mu\sin\phi}{2\pi a^2R^2s}\left(\pm\pi sx_<^2 + z\left[-3s^2E(m) + \big(4a^2+2R^2+3z^2\big)K(m) - \frac{(a-R)}{(a+R)}\big(a^2+R^2\big)\Pi(n|m)\right]\right) \tag{A6}$$

$$B_z = \frac{\mu\cos\phi}{\pi a^2Rst^2}\Big(\Big[a^2\big(R^2-z^2\big) - \big(R^2+z^2\big)^2\Big]E(m) + t^2\big(R^2+z^2\big)K(m)\Big) \tag{A7}$$

where ± is for $R \gtrless a$,

$$n = \frac{4aR}{(a+R)^2} \tag{A8}$$

$$m = \frac{4aR}{s^2} \tag{A9}$$

$$s = \sqrt{(a+R)^2+z^2} \tag{A10}$$

$$t = \sqrt{(a-R)^2+z^2} \tag{A11}$$

[39] $K(m)$, $E(m)$, and $\Pi(n|m)$ are complete elliptic integrals of the 1st, 2nd, and 3rd kinds, respectively (as defined in Mathematica http://www.wolfram.com), and $x_< = \min(a,R)$. For $z \gg a$ these reduce to a uniform field inside the Alfvén wing and a 2-d dipole field outside:

$$\mathbf{B} = \begin{cases} \dfrac{\mu}{a^2}\mathbf{e}_\mu & \text{for} \quad R < a,\ z \gg a \\ \dfrac{\mu}{R^2}\big(\sin\phi\mathbf{e}_\phi + \cos\phi\mathbf{e}_R\big) & \text{for} \quad R > a,\ z \gg a \end{cases} \tag{A12}$$

where $\mathbf{e}_\mu$ is a unit vector in the 2-d dipole direction.

[40] The total field is the sum of that from each Alfvén wing (north and south) and the current closing in the loops at the end of each cylindrical wing. The cylindrical coordinates are obtained by finding the nearest point to Galileo on each Alfvén characteristic, R being the distance from that point and z being the distance along the Alfvén characteristic of that point from the center of Io.

[41] **Acknowledgments.** This work was supported by NASA grant NNX06AB41G.

[42] Wolfgang Baumjohann thanks the reviewers for their assistance in evaluating this paper.

References

Acuña, M. H., and N. F. Ness (1976), The main magnetic field of Jupiter, *J. Geophys. Res.*, *81*, 2917–2922.

Acuña, M. H., F. M. Neubauer, and N. F. Ness (1981), Standing Alfvén wave current system at Io: Voyager observations, *J. Geophys. Res.*, *86*(A10), 8513–8521.

Bagenal, F. (1994), Empirical model of the Io plasma torus: Voyager measurements, *J. Geophys. Res.*, *99*(A6), 11,043–11,062.

Barbosa, D. D., A. Eviatar, and G. L. Siscoe (1984), On the acceleration of energetic ions in Jupiters magnetosphere, *J. Geophys. Res.*, *89*, 3789–3800.

Chenette, D. L., and L. Davis (1982), An analysis of the structure of Saturns magnetic field using charged particle absorption signatures, *J. Geophys. Res.*, *87*, 5267–5274.

Cohen, C. M. S., T. L. Garrard, E. C. Stone, J. F. Cooper, N. Murphy, and N. Gehrels (2000), Io encounters past and present: A heavy ion comparison, *J. Geophys. Res.*, *105*(A4), 7775–7782.

Cohen, C. M. S., E. C. Stone, and R. S. Selesnick (2001), Energetic ion observations in the middle Jovian magnetosphere, *J. Geophys. Res.*, *106*, 29,871–29,882.

Garrard, T. L., N. Gehrels, and E. C. Stone (1992), The Galileo heavy element monitor, *Space Sci. Rev.*, *60*, 305–315.

Garrard, T. L., E. C. Stone, and N. Murphy (1996), Effects of absorption by Io on composition of energetic heavy ions, *Science*, *274*, 393–394, doi:10.1126/science.274.5286.393.

Gehrels, N., and E. C. Stone (1983), Energetic oxygen and sulfur ions in the Jovian magnetosphere and their contribution to the auroral excitation, *J. Geophys. Res.*, *88*, 5537–5550.

Geiss, J., et al. (1992), Plasma composition in Jupiters magnetosphere: Initial results from the Solar Wind Ion Composition Spectrometer, *Science*, *257*, 1535–1539, doi:10.1126/science.257.5076.1535.

Hood, L. L. (1989), Radial diffusion in the Uranian radiation belts: Inferences from satellite absorption loss models, *J. Geophys. Res.*, *94*, 15,077–15,088.

Kivelson, M. G., F. Bagenal, W. S. Kurth, F. M. Neubauer, C. Paranicas, and J. Saur (2004), Magnetospheric interactions with satellites, in *Jupiter: The Planet, Satellites and Magnetosphere*, edited by F. Bagenal, T. E. Dowling, and W. B. McKinnon, pp. 513–536, Cambridge Univ. Press, New York.

Krimigis, S. M., et al. (1979a), Low-energy charged particle environment at Jupiter: A first look, *Science*, *204*, 998–1003, doi:10.1126/science.204.4396.998.

Krimigis, S. M., et al. (1979b), Hot plasma environment at Jupiter: Voyager 2 results, *Science*, *206*, 977–984, doi:10.1126/science.206.4421.977.

McKibben, R. B., K. R. Pyle, and J. A. Simpson (1983), Pioneer 11 observations of trapped particle absorption by Amalthea, *J. Geophys. Res.*, *88*(A1), 36–44.

Neubauer, F. M. (1980), Nonlinear standing Alfvén wave current system at Io: Theory, *J. Geophys. Res.*, *85*, 1171–1178.

Paranicas, C., and A. F. Cheng (1997), A model of satellite microsignatures for Saturn, *Icarus*, *125*(2), 380–396, doi:10.1006/icar.1996.5635.

Saur, J., F. M. Neubauer, D. F. Strobel, and M. E. Summers (2002), Interpretation of Galileos Io plasma and field observations: I0, I24, and I27 flybys and close polar passes, *J. Geophys. Res.*, *107*(A12), 1422, doi:10.1029/2001JA005067.

Selesnick, R. S. (1992), Magnetic field models from energetic particle data at Neptune, *J. Geophys. Res.*, *97*(A7), 10,857–10,863.

Selesnick, R. S. (1993), Micro- and macro- signatures of energetic charged particles in planetary magnetospheres, *Adv. Space Res.*, *13*(10), 221–230.

Thomsen, M. F. (1979), Jovian magnetosphere-satellite interactions: Aspects of energetic charged particle loss, *Rev. Geophys.*, *17*, 369–387.

Vogt, R. E., et al. (1979a), Voyager 1: Energetic ions and electrons in the Jovian magnetosphere, *Science*, *204*, 1003–1007, doi:10.1126/science.204.4396.1003.

Vogt, R. E., A. C. Cummings, T. L. Garrard, N. Gehrels, E. C. Stone, J. H. Trainor, A. W. Schardt, T. F. Conlon, and F. B. McDonald (1979b), Voyager 2: Energetic ions and electrons in the Jovian magnetosphere, *Science*, *206*, 984–987, doi:10.1126/science.206.4421.984.

C. M. S. Cohen, Space Radiation Laboratory, California Institute of Technology, MC 220-47, Pasadena, CA 91125, USA. (cohen@srl.caltech.edu)

R. S. Selesnick, P.O. Box 515381 #6702, Los Angeles, CA 90051-6681, USA. (rselesnick@gmail.com)